Biophysical Journal Volume 65 October 1993 1470–1485

Structural Heterogeneity of the Fe^{2+}-$N_\epsilon(His^{F8})$ Bond in Various Hemoglobin and Myoglobin Derivatives Probed by the Raman-active Iron Histidine Stretching Mode

Harald Gilch, Reinhard Schweitzer-Stenner,* and Wolfgang Dreybrodt
Fachbereich 1, Institute of Experimental Physics, University of Bremen, 28359 Bremen, Germany

ABSTRACT We have examined the Fe^{2+}-$N_\epsilon(His^{F8})$ complex in hemoglobin A (HbA) by measuring the band profile of its Raman-active $\nu_{Fe\text{-}His}$ stretching mode at pH 6.4, 7.0, and 8.0 using the 441-nm line of a HeCd laser. A line shape analysis revealed that the band can be decomposed into five different sublines at $\Omega_1 = 195\ cm^{-1}$, $\Omega_2 = 203\ cm^{-1}$, $\Omega_3 = 212\ cm^{-1}$, $\Omega_4 = 218\ cm^{-1}$, and $\Omega_5 = 226\ cm^{-1}$. To identify these to the contributions from the different subunits we have reanalyzed the $\nu_{Fe\text{-}His}$ band of the HbA hybrids $\alpha(Fe)_2\beta(Co)_2$ and $\alpha(Co)_2\beta(Fe)_2$ reported earlier by Rousseau and Friedman (D. Rousseau and J. M. Friedman. 1988. *In* Biological Application on Raman Spectroscopy. T. G. Spiro, editor. 133–216). Moreover we have reanalyzed other Raman bands from the literature, namely the $\nu_{Fe\text{-}His}$ band of the isolated hemoglobin subunits α^{SH}- and β^{SH}-HbA, various hemoglobin mutants (i.e., Hb($Tyr^{C7\alpha}\rightarrow$Phe), Hb($Tyr^{C7\alpha}\rightarrow$His), Hb M-Boston and Hb M-Iwate), *N*-ethylmaleimide-des($Arg^{141\alpha}$) hemoglobin (NES-des($Arg^{141\alpha}$)HbA) and photolyzed carbonmonoxide hemoglobin (Hb*CO) measured 25 ps and 10 ns after photolysis. These molecules are known to exist in different quaternary states. All bands can be decomposed into a set of sublines exhibiting frequencies which are nearly identical to those found for deoxyhemoglobin A. Additional sublines were found to contribute to the $\nu_{Fe\text{-}His}$ band of NES-des($Arg^{141\alpha}$) HbA and the Hb*CO species. The peak frequencies of the bands are determined by the most intensive sublines. Moreover we have measured the $\nu_{Fe\text{-}His}$ band of deoxyHbA at 10 K in an aqueous solution and in a 80% glycerol/water mixture. Its subline composition at this temperature depends on the solvent and parallels that of more R-like hemoglobin derivatives. We have also measured the optical charge transfer band III of deoxyHbA at room temperature and found, that at least three subbands are required to fit its asymmetric band shape. This corroborates the findings on the $\nu_{Fe\text{-}His}$ band in that it is indicative of a heterogeneity of the Fe^{2+}-$N_\epsilon(His^{F8})$ bond. Finally we measured the $\nu_{Fe\text{-}His}$ band of horse heart deoxyMb at different temperatures and decomposed it into three different sublines. In accordance with what was obtained for HbA their intensities rather than their frequencies are temperature-dependent. By comparison with $\nu_{Fe\text{-}His}$ bands of some Mb mutants (i.e., Mb($His^{E7}\rightarrow$Gly) and Mb($His^{E7}\rightarrow$Met) we suggest that these sublines may be attributed to different conformations of the heme pocket. Our data show, that the $\nu_{Fe\text{-}His}$ band is governed by at least two different coordinates *x* and *y* determining its frequency and intensity, respectively. While the former can be assigned to the tilt angle Θ between the Fe^{2+}-$N_\epsilon(His^{F8})$ bond and the heme normal and/or to the displacement δ of the iron from the heme plane, variations in the intensity may be caused by changes of the azimuthal angle ϕ formed by the projection of the proximal imidazole and the N(I)-Fe^{2+}-N(III) line of the heme. The sublines are therefore interpreted as resulting from different conformational substates of the Fe^{2+}-$N_\epsilon(His^{F8})$ complex which differ in terms of *x* (Θ and/or δ). Each of them may further be subdivided in sub-substates with respect to the coordinate *y* (ϕ). Quaternary and tertiary transitions of the protein alter the population of these substates thus giving rise to a redistribution of the $\nu_{Fe\text{-}His}$ sublines which shifts the corresponding peak frequency to higher values.

INTRODUCTION

The stretching mode of the Fe^{2+}-$N_\epsilon(His^{F8})$ bond ($\nu_{Fe\text{-}His}$) is Raman-active in the deoxy state of myoglobin, hemoglobin, and related model compounds. It exhibits a low frequency Raman band at about 216 cm^{-1} (Nagai et al., 1980; Hori and Kitagawa, 1980), which is significantly enhanced in the resonance region of the B-absorption band (Champion, 1988). As confirmed by numerous studies on the deoxygenated and photolyzed states of various myoglobin and hemoglobin derivatives its frequency is responsive to functionally relevant changes of the protein structure (Kitagawa, 1988; Rousseau and Friedman, 1988). In general the band shifts to higher frequencies when the protein changes from a T-like to a R-like structure. Matsukawa et al. (1984) showed a strong correlation between the peak frequency of the $\nu_{Fe\text{-}His}$ band and the first Adair constant. In accordance with other Raman data (Friedman, 1985) this shows that to a large extent the affinity of Fe^{2+} for the binding of O_2 and CO is determined by the conformation of the Fe^{2+}-His^{F8} complex.

Recently Bosenbeck et al. (1992) observed shifts of the $\nu_{Fe\text{-}His}$ band of deoxyhemoglobin trout IV (deoxyHb-trout IV) to higher frequencies upon variation of pH between 6 and 9. A line shape analysis revealed that this shift is caused by intensity variations of five different sublines (SLs) into which the band could be decomposed. Their frequencies were derived as $\Omega_1 = 202\ cm^{-1}$, $\Omega_2 = 211\ cm^{-1}$, $\Omega_3 = 217\ cm^{-1}$, $\Omega_4 = 223\ cm^{-1}$, and $\Omega_5 = 228\ cm^{-1}$ and do not depend on pH. The variation in their intensities

Received for publication 12 March 1993 and in final form 19 July 1993.

Address reprint requests to Reinhard Schweitzer-Stenner at the Institute of Experimental Physics-FB1, University of Bremen, 28359 Bremen, Germany. Tel.: 49-421-218-2509; Fax: 49-421-218-3601; e.mail: stenner@theo.physik.uni-bremen.de.

0006-3495/93/10/1470/16 $2.00

could be attributed to protonation of Bohr groups which were earlier derived from the respective O_2-binding isotherms (Schweitzer-Stenner and Dreybrodt, 1989). From the analysis of the different pH dependences of their intensities the SLs at Ω_1, Ω_2, Ω_3, were assigned to the α-, Ω_4, and Ω_5 of the β-subunits.

To elucidate the structural basis of their results Bosenbeck et al. (1992) employed a coupling model earlier proposed by Friedman and coworkers (Friedman et al., 1990; Ahmed et al., 1991). It assigns changes in frequency and intensity to variations of the polar angle Θ and azimuthal angle ϕ of the Fe^{2+}-His^{F8} complex, respectively. Using the concept of conformational substates as proposed by Frauenfelder et al. (1988), they assigned the observed SLs to conformations which differ in the tilt angle Θ. From the pH dependence of the SLs they inferred that due to protonation of Bohr groups a second configurational coordinate is activated. They proposed that this coordinate is the azimuthal angle ϕ, changes of which affect the intensity of the SLs, but leave its frequencies and, furthermore, the equilibrium between substates corresponding to them, unaffected. This suggests that the energy barriers between CS(Θ) are higher than those between CS(ϕ) and ranks the CS(Θ) to the tier CS^0 and CS(ϕ) to the tier CS^1 in the hierachy of CS as proposed by Ansari et al. (1985).

Structural heterogeneity in heme proteins has earlier been inferred from the band shape arising from the IR-active ν(C—O) mode of carbonmonoxide bound to the heme group. Makinen et al. (1979) have found, that for sperm whale myoglobin (Mb), this band can be decomposed into three different SLs. This observation was confirmed by Caughey et al. (1981) for bovine heart MbCO. By means of polarization experiments Ormos et al. (1988) related each SL to a distinct tilt angle between the CO-bond and the heme normal. These heme-ligand conformations were interpreted as substates of tier CS^0 (Ormos, et al., 1990). Jung and collaborators (Jung and Marlow, 1987; Jung, et al., 1992) found that the corresponding band of cytochrome $P450_{cam}$-CO can also be subdivided into SLs, the number of which changes when the substrate camphor is bound to the enzyme. The ν(C—O) band of bovine heart cytochrome oxidase was very recently found to consist of two comparatively sharp Sls (Tsubaki et al., 1992). Resonance Raman studies have further revealed that the band arising from the Raman-active v(Fe—C) vibration reflects the heterogeneity of the Fe—C—O complex in MbCO (Zhu et al., 1992; Srajer et al., 1986).

While the above experiments probe the heterogeneity of the distal side of the heme chromophore, the results of Bosenbeck et al. (1992) provide evidence, that in unligated hemoglobin the proximal side may also exist in different CS. For deoxyMb a similar message emerged from the analysis of the inhomogeneity of the Soret band (Srajer et al., 1986) and kinetic hole burning experiments on the absorption band III at 760 nm (Ahmed et al., 1991; Campbell et al., 1987; Chavez et al., 1990; Steinbach et al., 1991), which most probably arises from a $a_{2\,u}(P) \rightarrow d_\pi(Fe^{2+})$ charge transfer transition (Eaton et al., 1978). A decomposition of this band into different subbands, however, has not been performed in these investigations.

This study is aimed at obtaining more information on the conformational heterogeneity of the proximal Fe-His complex in human hemoglobin. To this end we measured the $\nu_{Fe\text{-}His}$ Raman band in deoxyHbA at different pH and temperatures and decomposed them into their SLs. It is well known that differences in the peak frequencies of the $\nu_{Fe\text{-}His}$ band exist (i) between the α- and β-subunits of deoxyHbA (Rousseau and Friedman, 1988; Ondrias et al., 1982), (ii) between unligated HbA in different quaternary states R and T (Kitagawa, 1988; Rousseau and Friedman, 1988; Friedman, 1985), and (iii) also between HbA at room and cryogenic temperature. In view of the results on Hb-trout IV (Bosenbeck et al., 1992) one may expect that these shifts can be explained in terms of variations in intensity of the underlying SLs rather than by shifts in frequency. To check this possibility we have reanalyzed line profiles of some $\nu_{Fe\text{-}His}$ bands reported in the literature: namely isolated HbA subunits (Nagai and Kitagawa, 1979), Fe/Co-hybrids, HbCO-photoproducts (Rousseau and Friedman, 1988), NES-des-($Arg^{141\alpha}$)-deoxyHbA (Kitagawa, 1988), and some deoxyHb mutants obtained by site directed mutagenesis (Nagai et al., 1989). To allow comparison with recent results on possible heterogenities in Mb we have also measured and analyzed the $\nu_{Fe\text{-}His}$ band of horse heart deoxyMb at various temperatures. Furthermore we reanalyzed the $\nu_{Fe\text{-}His}$ bands of Mb-($His^{E7} \rightarrow Gly$) and Mb($His^{E7} \rightarrow Met$) (Morikis et al., 1989). In addition we have measured and analyzed the profile of the charge transfer band III of deoxyHbA, which is expected to be sensitive to the proximal conformation of the heme (Campbell et al., 1987; Sassaroli and Rousseau, 1987; Chavez et al., 1990; Cordone et al., 1990; Srajer and Champion, 1991; Steinbach et al., 1992) and have found that this band can also be deconvoluted in subbands. The thus obtained results were then rationalized by means of two different models, which describe the relationship between the Fe^{2+}-His conformation and the frequency and intensity of the SLs.

MATERIALS AND METHODS

Preparation of the material

Hemoglobin A was prepared from freshly drawn blood by employing standard procedures (Spiro and Strekas, 1974). Horse heart myoglobin in lyophylized form was obtained commercially and was used without further purification. The pH value of the samples was adjusted by dialyzing against 0.05 M potassium phosphate buffer. The concentration (2 mM) of each sample was determined by measuring the absorbance with a HP-diode array spectrometer. By adding a few grains of sodium dithionite, each sample attained the deoxy state. To avoid oxygenation anaerobic conditions were maintained throughout the experiment.

Experimental set-up

The low frequency spectra of deoxyMb and deoxyHb (i.e., 100–400 cm^{-1}) were obtained using the 441-nm line of a HeCd laser (Omnichrome; Cinho,

CA) at an average power of 30 mW. Raman scattering was measured in the back-scattering configuration. The laser beam, polarized perpendicular to the scattering plane, was focussed by a cylindrical lense of 10-cm focal length onto the sample cuvette which was situated in a copper block for cooling. The scattered light was dispersed by a SPEX 1401 monochromator (SPEX Inds.; Edison, NJ). Most of the $\nu_{\text{Fe-His}}$ bands were recorded with a spectrometer speed of 0.03 cm^{-1}/s and a sampling time of 10 s. The spectral resolution was approximately 2.5 cm^{-1}.

For the experiments at cryogenic temperatures aqueous samples of deoxyHbA were placed into a low-temperature metacrylate cell with one quartz window. The cell was mounted to a cold finger of a Leybold-Heraeus closed-cycle refrigerator. The temperature was regulated by a Leybold-Controller unit. The sample was allowed to equilibrate 20 min at the indicated temperature. The aqueous solution was chosen to avoid interference of fluorescence which appears if the sample is dissolved in a glycerol-water solvent. The origin of this fluorescence is still to be resolved. Since its intensity is sufficiently low in the low frequency region of Raman spectra measured at low cryogenic temperatures, we also managed to measure the $\nu_{\text{Fe-His}}$ band profile of deoxyHbA in 80% glycerol/water at T = 10K.

The optical band III was measured using a Shimadzu dual wavelength double beam spectrophotometer with a resolution of 2 nm. For this experiment deoxyHbA was dissolved in a 65% glycerol/water mixture. The concentration was 1.4 mM.

Analysis of the line profiles

The line profiles of the $\nu_{\text{Fe-His}}$ bands were analyzed by using the program SpectraCalc purchased from Photometrix (Munich, Germany) subtracting the (Rayleigh) background and decomposing the profile alternatively into Lorentzian or Gaussian SLs with adjustable frequencies, halfwidths, and heights. In both cases high quality fits to the entire band profile were obtained. The frequencies of the SLs and their intensities do not significantly depend on the line form used for the fits. The frequency values were determined by use of the plasma line at 441.6 nm of the HeCd laser which appeared in the Raman spectrum at 282.8 cm^{-1}. The error of the derived frequencies of the SLs was ± 1 cm^{-1}. A detailed description of the fitting strategy is given in the next section.

To investigate the reliability of the fits we employed a method proposed by Grinvald and Steinberg (1974), who used the autocorrelation function of the residuals of a fit to judge its quality. This function $C(\Omega)$ is given by

$$C(\Omega_j) = \frac{1}{m}\sum_{i=1}^{m}(\delta_i\delta_{i+j}) \Bigg/ \left(\frac{1}{n}\sum_{i=1}^{n}\delta_i^2\right) \qquad (1)$$

$\delta_i = S(\Omega_i) - S_{\text{exp}}(\Omega_i)$ is the difference between the fit function and the experimentally observed value $S_{\text{exp}}(\Omega_i)$ at wavenumber Ω_i. n is the number of points and $m = n/2$. The autocorrelation function thus defined contains high frequency fluctuations, due to the noise in the spectra and low frequency deviations about zero due to systematic nonrandom deviations between the fit function and the real physical wavenumber dependence of the Raman band.

RESULTS AND DISCUSSION

Experiments on deoxyHbA at room temperature

The $\nu_{\text{Fe-His}}$ bands of deoxyHbA have been measured at room temperature and at various pH. A typical line profile of deoxyHbA at pH 6.4 is shown in Fig. 1 *a*. At the low frequency side of the band *a* shoulder is clearly visible, which becomes less pronounced with increasing pH at pH 7 (Fig. 1 *b*) and is further reduced at pH 8.0 (Fig. 1 *c*), where only an asymmetric shape of the band remains (Fig. 1 *c*). These data indicate that the band profile is a superposition of several SLs.

In order to find a numerical expression, which gives a optimal fit to the data we adopted the following protocol: In a first step we try to fit the data with only one line, using a Lorentzian with frequency position Ω_1, amplitude A_1, and halfwidth Γ_1 as fitting parameters. In the next step, we use two independent Lorentzians with the frequencies Ω_1, Ω_2, and amplitudes A_1, A_2. The two halfwidths Γ_1 and Γ_2 were kept equal within ± 2.0 cm^{-1}, because in the absence of further inhomogenous broadening sublines resulting from the same normal mode can be expected to have similar halfwidths. This is repeated correspondingly with 3, 4, etc. Lorentzians until no further improvement of the fit is obtained. Now for each of these fits the autocorrelation function $C_k(\Omega_j)$ is computed (Eq. 1, k is the number of Lorentzians used). In a final step we calculated the differences $C_{k+1}(\Omega_j) - C_k(\Omega_j)$, which are displayed in Fig. 2. By this procedure the random noise contributions are eliminated, and only the

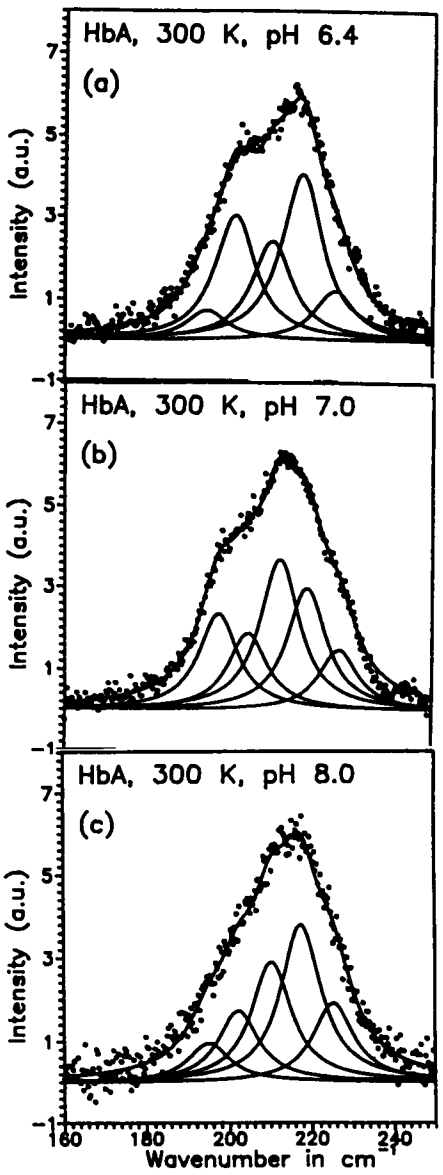

FIGURE 1 Band profiles of the $\nu_{\text{Fe-His}}$ band of deoxyHbA at pH 6.4 (*a*), 7.0 (*b*), and 8.0 (*c*) in a 0.05 M phosphate buffer. The profile was decomposed into five different sublines displayed by solid lines. The band profile was measured as described under Materials and Methods.

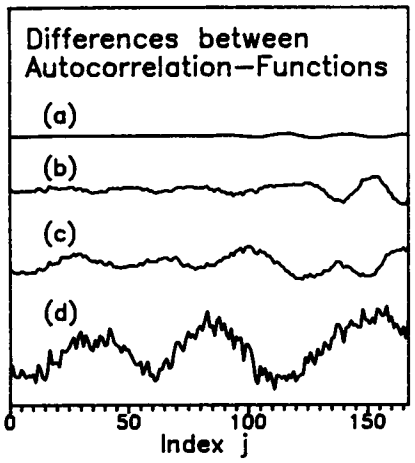

FIGURE 2 Plot of the differences between the autocorrelation functions obtained from the fits to the band profile in Fig. 1 *c* using 1 and 2 (*d*), 2 and 3 (*c*), 4 and 5 (*b*), 5 and 6 (*a*) Lorentzian sublines. The autocorrelation function has been calculated by use of Eq. 1. The indices j from 0 to 174 cover the spectral region between 160 and 260 cm^{-1}.

systematic deviations due to the imperfect fitting function remain. Increasing the number of lines yields smaller differences until at a distinct number k^* no further improvement is obtained.

As shown in Fig. 1, *a–c*, all these bands could be fitted with a minimal number of five SLs with corresponding frequencies and halfwidths (cf. the line parameters listed in Table 1). They are designated as SL_1 (Ω_1 = 196 ± 1 cm^{-1}), SL_2 (Ω_2 = 203 ± 1 cm^{-1}), SL_3 (Ω_3 = 211 ± 1 cm^{-1}), SL_4 (Ω_4 = 218 ± 1 cm^{-1}), and SL_5 (Ω_5 = 226 ± 2 cm^{-1}). The intensities of the SLs, however, depend on pH, such that the lines with higher frequencies gain more intensity at higher pH. These data unambiguously show that the $\nu_{Fe\text{-}His}$ bands in Fig. 1, *a–c*, are not homogenous but exhibit structural inhomogeneity, which is altered upon changes of pH.

TABLE 1 Band parameters derived from the analysis of $\nu_{Fe\text{-}His}$ of deoxyHbA at pH 6.4, 7.0, and 8.0

j	pH	Ω_j	Γ_j	I_j/I_T
		cm^{-1}	cm^{-1}	
1	6.4	195	12.0	0.06
	7.0	198	11.7	0.19
	8.0	195	12.0	0.08
2	6.4	202	12.0	0.27
	7.0	205	11.7	0.15
	8.0	202	12.0	0.15
3	6.4	211	12.0	0.21
	7.0	213	11.7	0.30
	8.0	211	12.0	0.23
4	6.4	218	12.0	0.35
	7.0	219	11.7	0.24
	8.0	218	12.0	0.35
5	6.4	226	12.0	0.11
	7.0	227	11.7	0.12
	8.0	226	12.0	0.19

I_j, intensity of the jth SL; I_T, total intensity.

In principle the position of SLs can be obtained from the minima of the second derivative of the band shape. In our case the low signal to noise ratio of the $\nu_{Fe\text{-}His}$ band makes this procedure cumbersome. It is interesting, however, to compare the second derivatives of the fitted and the experimental band shape. Fig. 3 shows that they exhibit minima at nearly the same wavenumber positions. This finding further supports the result of our analysis.

The pH dependence of $\nu_{Fe\text{-}His}$ is in contrast to results earlier obtained from measurements of the $\nu_{Fe\text{-}His}$ band of deoxyHbA (Bosenbeck et al., 1992), which indicated that heme-protein coupling in this molecule does not depend on pH between 6 and 9. In the present study, however, we have used phosphate buffer to adjust pH in order to allow comparison with measurements at cryogenic temperatures, which will be discussed below. For these experiments, phosphate buffer is more convenient than the bis-tris and tris buffer employed in the above study. Since functionally relevant interactions occur between phosphate binding sites and the heme and phosphate and H^+ binding sites in the protein (Russu et al., 1989; Chiancome et al.; 1983), the pH dependence of the $\nu_{Fe\text{-}His}$ band in reality may be caused by the phosphate binding to specific amino acid residues, the binding affinity of which is modulated by the protonation of nearby side chains. This interpretation is confirmed by recent experiments in our laboratory which show that the $\nu_{Fe\text{-}His}$ band is indeed practically pH-independent if the deoxyHb is dissolved in bis tris/tris buffer of low ionic strength ($Cl^- < 0.1$ M).

In the present study, however, it is only relevant to note that this band exhibits heterogeneity. This is in particular judged by the different asymmetries of the band profiles in Fig. 1, *a–c*.

Analysis of $\nu_{Fe\text{-}His}$ bands reported in the literature

a) $\nu_{Fe\text{-}His}$ in the spectrum of chemically modified Hb

It is well known from a large number of experimental data, that the $\nu_{Fe\text{-}His}$ band shows a shift of its peak frequency to

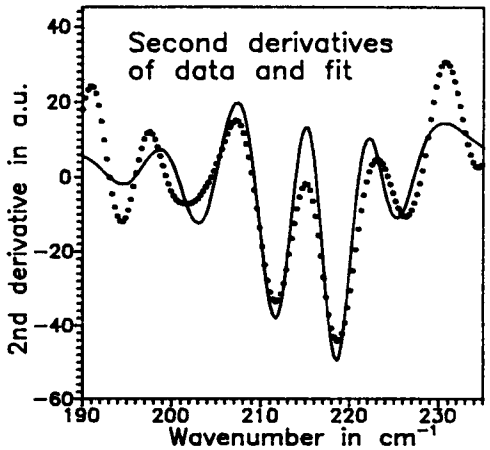

FIGURE 3 Second derivative of the experimental (*dotted line*) and fitted $\nu_{Fe\text{-}His}$ band profile in Fig. 1 *c* (*solid line*).

higher values when the quaternary structure of Hb becomes more R-like. Thus $\nu_{Fe\text{-}His}$ of the T-state deoxyHbA exhibits a peak frequency of about 215 cm^{-1}, whereas the corresponding peak frequency of R-state like modified NES-des-($Arg^{141\alpha}$)-deoxyHbA is at 224 cm^{-1}. To elucidate this behavior in terms of structural heterogeneity, we have decomposed the $\nu_{Fe\text{-}His}$ band of a variety of modified deoxyHbA species, which have been published in the literature. Fig. 4 shows the decomposition of NES-des($Arg^{141\alpha}$)-deoxyHb (data taken from Kitagawa (1988)). The band can be decomposed into 4 SLs, where the frequencies of SL_2, SL_3, SL_4, and SL_5 are close to those of SL_2 to SL_5 in deoxyHbA (cf. Table 2), whereas SL_1 is absent. The apparent shift of the peak frequency of this band compared to its deoxyHbA position is caused by an increase of the intensities of the SLs at higher frequencies. As a consequence the intensity ratio of SL_4 to SL_5 is almost reversed in comparison to deoxyHbA.

b) $\nu_{Fe\text{-}His}$ in the spectra of transient species

When HbCO is photolyzed, the heme group switches into a deoxy-like conformation in less than 1 ps (Terner et al., 1980). After this time the iron atom is displaced from the heme plane (defined by the pyrrole nitrogens) by about 0.2–0.3 Å, but the Fe-N_ϵ(His^{F8}) bond remains nearly parallel to the heme normal (Rosseau and Friedman, 1988). After this event the protein rearranges its structure. The subunits switch from their r- to the corresponding t-states on the nanosecond time scale (Friedman, 1985) and subsequently the quaternary structure undergoes its R→T transition on a microsecond time scale (Rodgers et al., 1992). This causes a larger tilt of the Fe-N_ϵ(His^{F8}) bond and increases the Fe^{2+} displacement to the final value of ≈0.38 Å. We have analyzed the transient $\nu_{Fe\text{-}His}$ signal of Hb*CO occurring within 25 ps after photolysis and also the transient signal, which is obtained after 10 ns (Rousseau and Friedman, 1988). The results are illustrated by Fig. 5. In the 25-ps band we observed the lines SL_4, SL_5, SL_6, and new lines (SL_7) at 240 cm^{-1} and SL_8 at 248 cm^{-1}. The band profile observed after 10 ns exhibits SL_3, SL_4, SL_5, and SL_6 and thus shows a rearrangement to conformations at lower frequencies, indicating continued relaxation toward the T-state. The band parameters obtained from the fits are listed in Table 2.

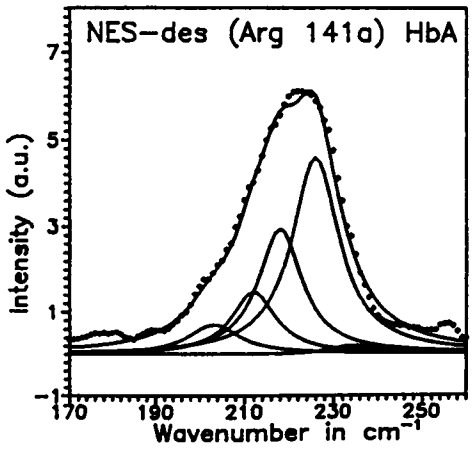

FIGURE 4 Band profiles of the $\nu_{Fe\text{-}His}$ band of NES-des($Arg^{141\alpha}$)deoxyHbA taken from Kitagawa (1988). The profile was decomposed into five different sublines displayed by solid lines.

TABLE 2 Band parameters derived from the analysis of $\nu_{Fe\text{-}His}$ of NES-des($Arg^{141\alpha}$)-deoxyHbA and the transient species Hb*CO obtained 25 ps and 10 ns after photolysis of CO

Hb-type	j	Ω_j	I_j/I_T
		cm^{-1}	
NES-des($Arg^{141\alpha}$)	1		
	2	203	0.08
	3	212	0.14
	4	218	0.28
	5	225	0.48
	6	234	0.02
	7		
Hb*CO (25 ps)	1		
	2		
	3	212	0.04
	4	218	0.15
	5	226	0.21
	6	232	0.38
	7	242	0.13
	8	248	0.09
Hb*CO (10 ns)	1		
	2		
	3	211	0.08
	4	219	0.28
	5	226	0.50
	6	235	0.14
	7	241	

I_j, intensity of the jth SL; I_T, total intensity, the halfwidths Γ_j varied between 12 and 14 cm^{-1}.

c) $\nu_{Fe\text{-}His}$ in the spectra of Hb mutants

As a further example we have decomposed the $\nu_{Fe\text{-}His}$ bands of two HbA mutants, in which $Tyr^{C7\alpha}$ was replaced by Phe (Hb($Phe^{C7\alpha}$)) and by His (Hb($His^{C7\alpha}$)) by virtue of site-directed mutagenesis (Nagai et al., 1991). These substitutions are functionally significant, because $Tyr^{C7\alpha}$ donates a hydrogen bond to Asp G1β which stabilizes to a large extent the deoxy T structure (Perutz, 1989). This intersubunit contact is absent in Hb(Phe^{C7}) and replaced by a weaker hydrogen bond in Hb(His^{C7}). Consequently the T-state is destabilized in both molecules, thus increasing the ligand binding affinity and decreasing cooperativity. Therefore the deoxygenated quaternary state of both molecules may be regarded as more R-like. This is also reflected by the results emerging from the decomposition of their $\nu_{Fe\text{-}His}$ bands (Fig. 6). The frequencies of SL_1–SL_5 are equal to the those obtained for the corresponding SLs of deoxyHbA (Table 3). In addition a weak SL_6 appears in the band of Hb($His^{C7\alpha}$). The more R-like structure of Hb(PheC7α) is reflected by the stronger intensity of its Sl_5 in comparison to Hb($His^{C7\alpha}$).

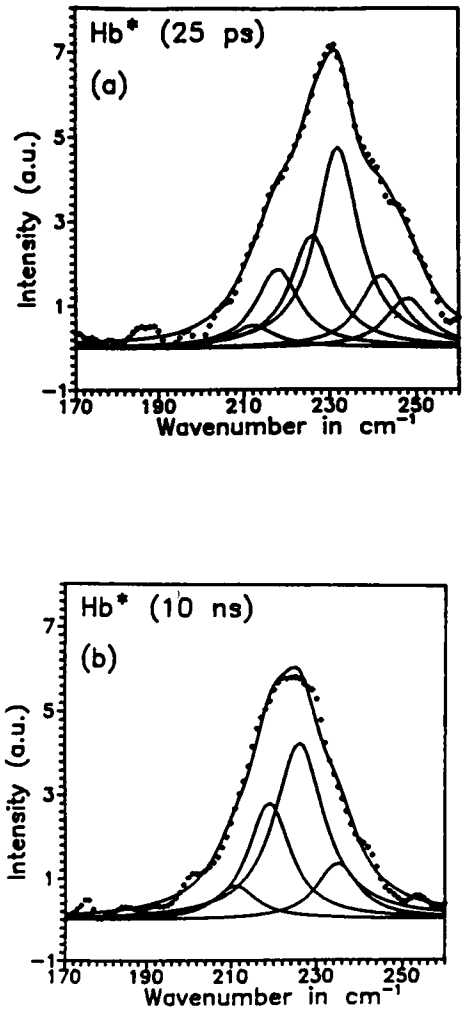

FIGURE 5 Band profiles of the $\nu_{Fe\text{-}His}$ band of Hb*CO 25 ps (*a*) and 10 ns (*b*) after photolysation. The data were taken from Rousseau and Friedman (1988). The profile was decomposed into five different sublines displayed by solid lines.

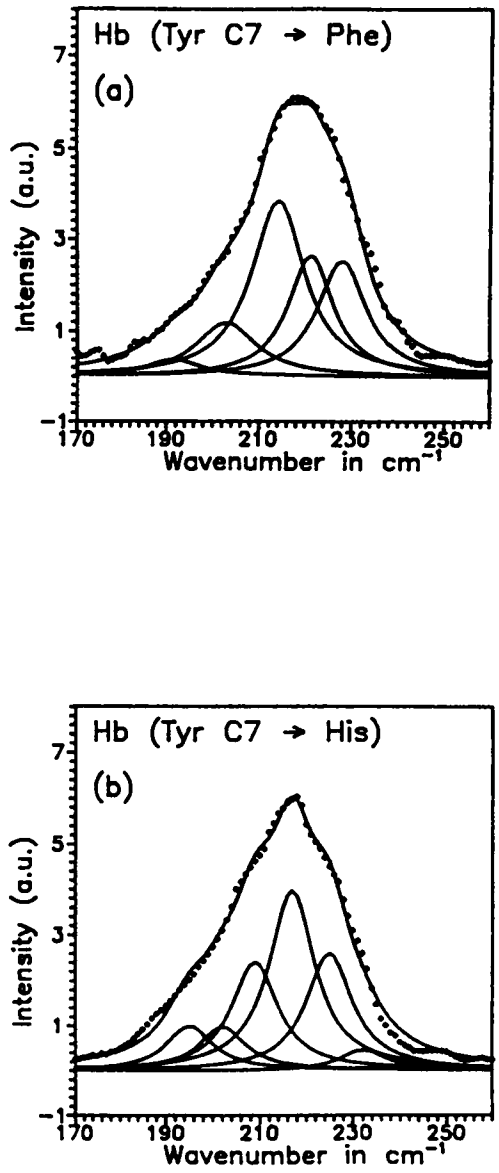

FIGURE 6 Band profiles of the $\nu_{Fe\text{-}His}$ bands of Hb(Phe^{C7} (*a*) and Hb (His^{C7}) (*b*). The data were taken from Nagai et al. (1991). The profiles were decomposed into six sublines displayed by solid lines.

All these findings on more R-like hemoglobin derivatives suggest the following picture for the description of T→R transitions. Each of these quaternary states consists of several $CS_j(x)$, where x is a conformational coordinate which gives rise to different conformations of the Fe-N_ϵ(His^{F8}) complex. Since the intensities rather than the frequencies of the SLs change significantly upon the quaternary T→R switch, we conclude that corresponding $CS_j(x)$ in T and R exhibit nearly the same structure with respect to the protein coordinate x but have different intensities. Thus the T→R transition causes changes in SL intensities related to the CS of the Fe^{2+}-His^{F8} linkage. Theses changes in intensity can result from a redistribution within these substates, but it is also possible that redistribution between the substates along another conformational coordinate y exists, which affects solely the intensity of the SLs.

To confirm this interpretation we have analyzed a variety of Fe-His band shapes of HbA mutants (HbM) reported in the literature, namely HbM-Boston ($His^{E7\alpha}$→Tyr), HbM-Iwate ($His^{F9\alpha}$→Tyr) (Nagai et al., 1989), and HbJ-Capetown ($Arg^{FG4\alpha}$→Glu) (Matsukawa et al., 1984) (data not shown). The thus derived band parameters are listed in Table 3, together with the other Hb derivatives discussed above. Fig. 7 shows a graphical representation of the observed SLs with respect to their frequencies and intensities. Clearly all line profiles could be decomposed into very similar sets of SLs with respect to their frequencies (and not shown in Fig. 7, also with respect to their halfwidths). The different shapes of the $\nu_{Fe\text{-}His}$ bands result from the differing intensities of these SLs, indicating that both, conformational changes within T and R and the T→R transition itself cause a rearrangement of the distribution between the corresponding $CS_j(x)$.

TABLE 3 Band parameters derived from the analysis of $\nu_{Fe\text{-}His}$ of the deoxyHbA mutants Hb(Phe$^{C7\alpha}$), Hb(His$^{C7\alpha}$), Hb M-Boston, Hb M-Iwate, and Hb J-Captetown

Hb-type	j	Ω_j	I_j/I_T
		cm^{-1}	
Hb(Phe$^{C7\alpha}$)	1	191	0.04
	2	203	0.13
	3	214	0.38
	4	221	0.22
	5	228	0.23
	6		
Hb(His$^{C7\alpha}$)	1	195	0.08
	2	202	0.09
	3	209	0.21
	4	217	0.35
	5	225	0.23
	6	233	0.04
	7		
Hb M-Boston	1	194	0.12
	2	204	0.18
	3	212	0.31
	4	219	0.30
	5	224	0.08
	6		
	7		
Hb M-Iwate	1	200	0.07
	2	205	0.14
	3	211	0.17
	4	216	0.22
	5	222	0.40
	6		
	7		
Hb J-Capetown	1	196	0.08
	2	204	0.14
	3	210	0.16
	4	218	0.32
	5	225	0.23
	6	232	0.06

Definitions same as in Tables 1 and 2.

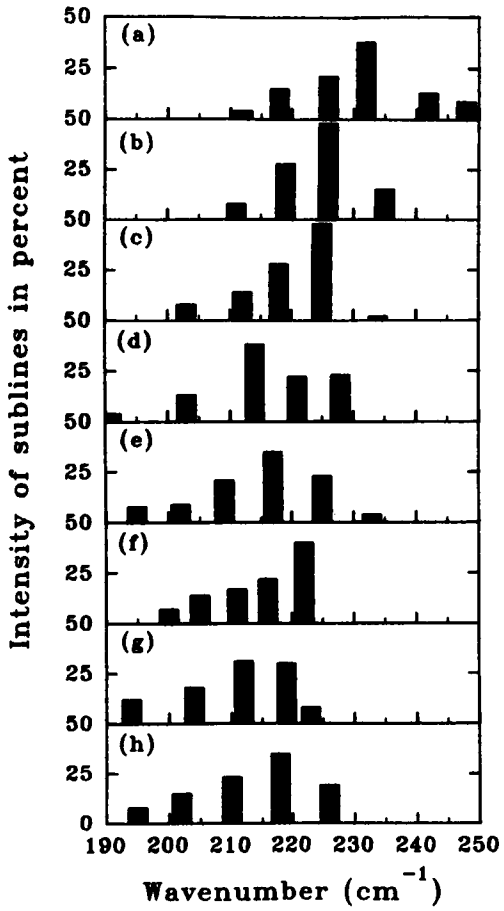

FIGURE 7 Representation of frequencies and intensities of the sublines derived from the fits to HbA (*a*) Hb$^{\bullet}$CO 25 ps and (*b*) 10 ns after photolysis, (*c*) NES-des(Arg$^{141\alpha}$)deoxyHbA, (*d*) Hb(Phe$^{C7\alpha}$), (*e*) Hb(His$^{C7\alpha}$), (*f*)Hb-Iwate, (*g*) Hb M-Boston, and (*h*) deoxyHbA. Spectra at the top reflect a more R-like and at the bottom a more T-like structure of the protein.

d) $\nu_{Fe\text{-}His}$ in the spectra of isolated subunits and Hb hybrids

It is well known that the structure of the heme-His^{F8} linkage is different in the α- and β-chains of deoxyHbA (Fermi et al., 1984). One may therefore suspect that an inhomogenous band shape of the $\nu_{Fe\text{-}His}$ mode may also result from differences in the force constants of the Fe^{2+}-N_ϵ(His^{F8}) bonds in these subunits. Indeed earlier studies revealed that their $\nu_{Fe\text{-}His}$ bands exhibit different peak frequencies (Ondrias et al., 1982). We have therefore analyzed the $\nu_{Fe\text{-}His}$ bands in the spectra of isolated α- and β-chains of deoxyHbA (α^{SH}-HbA, β^{SH}-HbA) (Nagai and Kitagawa, 1979) and also of the tetrameric hybrids $\alpha(Fe)_2\beta(Co)_2$-Hb and $\alpha(Co)_2\beta(Fe)_2$-Hb (Rousseau and Friedman, 1988). The frequencies and intensities of the SLs are listed in Table 4. As shown in Fig. 8 all band shapes can be fitted by the same set of SLs used to fit the corresponding band profiles of deoxyHbA and its derivatives. By comparing the data of α^{SH}- and β^{SH}-HbA one finds the most intensive SLs at 223 cm^{-1} (SL_4) and 230 cm^{-1} (SL_5). In the low frequency region (Ω_2, Ω_3) the SLs of α^{SH}-HbA are stronger than those of β^{SH}-HbA. The β-chain exhibits weak shoulders at Ω_6 and Ω_7 (235 and 243 cm^{-1}). The latter is absent in the spectrum of the α-chain.

Compared to isolated α^{SH}-HbA the α-subunit in $\alpha(Fe)_2\beta(Co)_2$ shows a rearrangement of intensities to the SLs at lower frequencies. This is also the case for the β-subunits in $\alpha(Co)_2\beta(Fe)_2$ in comparison to β^{SH}-HbA. This indicates to the fact that the quaternary structure imposes steric restrictions on the Fe^{2+}-N_ϵ(His^{F8}) bonds, rendering them more t-like in comparison to the isolated chains. Apparently the β-subunits are in a more r-like conformation than the α-chains.

To summarize so far we state that the existence of structural heterogeneity of the $\nu_{Fe\text{-}His}$ band can be inferred from the data for both, the α- and β-subunits. Five conformations exist in the tertiary t-state which are characterized by their frequencies, but show varying intensities in various proteins.

Deoxyhemoglobin at cryogenic temperatures

As discussed above, the heterogeneity of the $\nu_{Fe\text{-}His}$ band can be interpreted by attributing its SLs to different CS(x) with respect to a still unknown protein coordinate x. Thus our data

TABLE 4 Band parameters derived from the analysis of $\nu_{Fe\text{-}His}$ of α^{SH}-HbA, β^{SH}-HbA, $\alpha(Fe)_2\beta(Co)_2$Hb and $\alpha(Co)_2\beta(Fe)_2$Hb

Hb-type	j	Ω_j	I_j/I_T
		cm^{-1}	
α^{SH}-HbA	1	194	0.04
	2	204	0.10
	3	212	0.17
	4	219	0.21
	5	225	0.29
	6	235	0.19
	7		
β^{SH}-HbA	1		
	2		
	3	212	0.02
	4	218	0.12
	5	226	0.53
	6	235	0.31
	7	243	0.02
$\alpha(Fe)_2\beta(Co)_2$HbA	1	195	0.20
	2	203	0.38
	3	212	0.22
	4	218	0.20
	5	225	0.01
	6	235	
	7	243	
$\alpha(Co)_2\beta(Fe)_2$HbA	1		
	2	202	0.03
	3	210	0.31
	4	218	0.39
	5	226	0.27
	6		
	7		

I_j, intensity of the j th SL; I_T, total intensity; the halfwidths Γ_j varied between 12 and 14 cm^{-1}.

corroborate the concept of structural heterogeneity in proteins proposed by Frauenfelder, Parak, and coworkers (cf. Frauenfelder et al., 1988). From a large body of investigations on the structure and function of myoglobin they provided evidence that this protein can exist in numerous CS that perform the same function but with different rates. Moreover it was proposed that the CS are arranged in a hierachy of several tiers (Ansari et al., 1985). At physiological temperature the protein fluctuates among the substates of all tiers. As the temperature is lowered, the CS belonging to different tiers freeze out subsequently. The CS^0 of the upper tier, for instance, freeze out at about 180 K, if the protein is in a glycerol-water solvent (Ansari et al., 1987). Other experiments suggest a glass-like behaviour of the protein with a transition temperature at 185 K (Iben et al., 1989; Doster et al., 1989; Nienhaus et al., 1989; Nienhaus et al., 1992). Recent molecular dynamics studies on Mb by Elber and Karplus (1987) revealed the existence of more than 2×10^3 CS, which are involved in fluctuations proceeding on a time scale of up to 300 ps. Slower motions affecting the heme iron were detected by Mößbauer spectroscopy on deoxyMb and deoxyHb (Frauenfelder et al., 1988; Parak et al., 1982; Mayo et al., 1983). Now the question arises, whether the CS reflected by the SLs of the $\nu_{Fe\text{-}His}$ band exhibit a similar behavior as those derived from the studies by Frauenfelder and coworkers. To address this point we have measured the $\nu_{Fe\text{-}His}$ band of deoxyHbA at 10 k. Fig. 9 shows the band shapes of a frozen aqueous solution (9 *a*) and a glycerol-water mixture (80%) (9b). The latter data set is obscured by large noise caused by the fluorescence background. For the sample in aqueous solution the band analysis yields SLs at $\Omega_4 = 218\ m^{-1}$, $\Omega_5 = 226\ cm^{-1}$, $\Omega_6 = 233\ cm^{-1}$, and $\Omega_7 = 240\ cm^{-1}$ (the label of the SLs follows the assignment made above for the deoxyHbA-SLs measured at room temperature). The peak intensity is determined by Ω_6 (cf. the band parameters in Table 5). This suggests that a lowering of temperature depopulates the CS(x) reflected by SL_1, SL_2 and SL_3. Surprisingly, SLs which are absent at room temperature, i.e., SL_6 and SL_7, show up at 10 K. Taking into account our results on the R-like deoxyHb derivatives one suspects that lowering of the temperature shifts the protein into a more R-like conformation. A better understanding of this observation requires knowledge of the temperature dependence of the SL intensities. This is currently under investigation in our laboratory.

First measurements at room temperature show, that the $\nu_{Fe\text{-}His}$ bands measured in an aqueous solution and in 80% glycerol-water mixture are practically identical. Thus they can be decomposed into the same SLs. At $T = 10$ K, however, the SLs derived from $\nu_{Fe\text{-}His}$ band measured with a glycerol-water solution (Fig. 9 *b*) exhibit frequencies at $\Omega_1 = 195\ cm^{-1}$, $\Omega_2 = 202\ cm^{-1}$, $\Omega_4 = 218\ cm^{-1}$, $\Omega_5 = 225\ cm^{-1}$, $\Omega_6 = 235\ cm^{-1}$, and $\Omega_7 = 242\ cm^{-1}$ (cf. Table 5). Only Sl_3 at $211\ cm^{-1}$ is absent. The low frequency side of the $\nu_{Fe\text{-}His}$ band, however, becomes more pronounced in a glycerol water solution. This holds especially for SL_1, which is weak at room temperature but contributes significantly to the band shape at cryogenic temperatures. Thus it becomes apparent that in this temperature regime interaction between a glass like solvent (i.e., glycerol-water), and the protein may have a major influence on the CS involved in the Fe-His^{F8} linkage.

Comparison with myoglobin

Most of the experiments dedicated to explore CS of heme proteins were carried out on monomeric systems, i.e., myoglobin (Frauenfelder et al., 1988) and cytochrome P450 (Jung and Marlow, 1987; Jung et al., 1992). Even though this study is aimed at getting information on the CSs in hemoglobin, it is useful to examine the $\nu_{Fe\text{-}His}$ band of myoglobin. Therefore we have measured the corresponding band profile of horse heart deoxyMb at pH 7.5 at various temperatures and subjected the data to a band profile analysis. Some results are displayed in Fig. 10. All three band profiles at 300, 150, and 10 K can be decomposed into a common set of five SLs at 196, 208, 216, 225, and 240 cm^{-1} (parameter values are given in Table 6). Whereas the two lines at the high and low energy wings of the bandshape are relatively insensitive to changes in temperature, the three central lines exhibit a dramatic change in their intensities with decreasing temperature. The fractional intensity of the SL at 229 cm^{-1} (SL_{Mb3}) increases by roughly a factor of 2 in its intensity from 300 K down to 10 K. In contrast the corresponding intensity of the line at 216

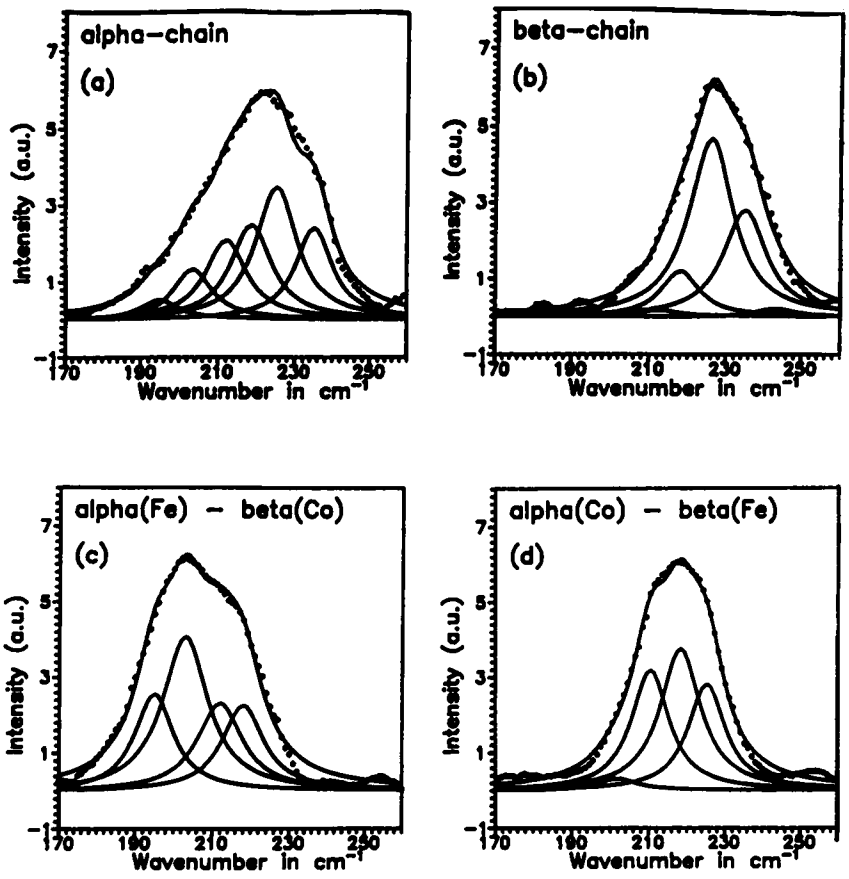

FIGURE 8 Band profiles of the $\nu_{Fe\text{-}His}$ bands of α^{SH}-HbA (*a*), β^{SH}-HbA (*b*), $\alpha(Fe)_2\beta(Co)_2$HbA (*c*), and $\alpha(Co)_2\beta(Fe)_2$HbA (*d*) (data from Kitagawa (1988) and Rousseau and Friedman (1988). The profiles were decomposed into different sublines by solid lines.

cm^{-1} (SL_{Mb2}) decreases by almost a factor of 3. The weak line at 208 cm^{-1} (SL_{Mb1}) vanishes completely at 10 K. We assign these three lines to the Fe^{2+}-N_ϵ(His^{F8}) stretching mode in different conformational configurations. The line at 240 cm^{-1} is known to result from a pyrrole rocking mode (Rousseau and Friedman, 1988). Its insensitivity to temperature below 150 K makes it a good standard to the reliability of the decomposition of the $\nu_{Fe\text{-}His}$ band shape. The line at 195 cm^{-1} seems to be different from the corresponding line at the same wavenumber position on the HbA spectrum. Its origin is still unclear.

From these data we conclude that myoglobin also exists in conformational substates with respect to the Fe—His bond. Similarly as in Hb the high frequency components of the SLs determine the spectra at low temperature, indicating that the corresponding CS may be significantly determined by the tertiary structure of the proteins.

Further information on the relationship between the above SLs and differences in the tertiary structure can be derived from the $\nu_{Fe\text{-}His}$ band of some Mb mutants, in which the distal histidine E7 is replaced by another ligand. Fig. 11 displays the $\nu_{Fe\text{-}His}$ band shape of native sperm whale deoxyMb (Fig. 11 *a*) and its mutants Mb(Gly^{E7}) (11 *b*) and Mb(Met^{E7}) (11 *c*, data from Morikis and Champion, 1989). The subline spectrum of sperm whale Mb is similar to that of horse heart Mb (Fig. 10), but exhibits a more predominant SL_{Mb2} (cf. also the band parameters given in Table 6). The low frequency mode at 196 cm^{-1} is absent. As shown in Fig. 11, *a* and *c*, the SL spectrum of the above mutants differ significantly from that of the native molecule. In Mb(Met^{E7}) SL_{Mb2} and SL_{Mb3} exhibit similar intensities, whereas SL_{Mb3} becomes superior in Mb(Gly^{E7}). This shows that changes in the distal part of the heme pocket affect the equilibrium between different CS of the proximal side to a significant extent, in contrast to what has been inferred from the same data set by Morikis and Champion (1989).

It is interesting to compare these findings with the results emerging from the analysis of the Raman and IR band arising from the CO-stretching mode of heme bound CO. Ansari and coworkers (1987) found that the IR band can be decomposed into four different SLs termed A_0, A_1, A_2, and A_3 (A_2 was neglected in later investigations of this band). At room temperature and physiological pH A_1 is predominant. The ratios of the corresponding extinctions A_0/A_1 and A_3/A_1 were found to be 0.13 and 0.33, respectively. The Raman band exhibits similar intensity ratios, i.e., $A_0/A_1 = 0.06$ and $A_3/A_1 = 0.37$. In Mb(Gly^{E7}), however, A_0/A_1 is 1.9 and A_3 is not detectable (Morikis and Champion, 1989). These results compare with the corresponding $\nu_{Fe\text{-}His}$ Raman data in the following way. Using the parameters in Table 6 we obtain the intensity ratios $I(SL_{Mb3})/I(SL_{Mb2}) = 0.32$ and $I(SL_{Mb1})/I(SL_{Mb2}) = 0.11$ for native Mb and $I(SL_{Mb3})/I(SL_{Mb2}) = 1.8$ and $I(Sl_{Mb1})/I(SL_{Mb2}) = 0.11$ for Mb(Gly^{E7}). Taken together these values

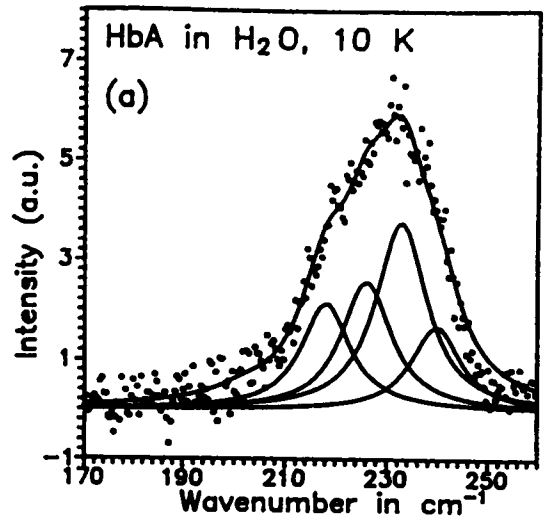

FIGURE 9 Band profiles of the $\nu_{Fe\text{-}His}$ bands of deoxyHbA measured at 10 K in an aqueous solution (*a*) and in a 80% glycerol/water mixture (*b*) as described under Material and Methods. The profiles were decomposed into four and six different sublines displayed by solid lines.

TABLE 5 Band parameters derived from the analysis of $\nu_{Fe\text{-}His}$ of deoxyHbA measured at 10 K in an aqueous and 80% glycerol/water solution

Hb-type	j	Ω_j	I_j/I_T
		cm^{-1}	
DeoxyHbA in H_2O	1		
	2		
	3	202	0.01
	4	218	0.21
	5	226	0.25
	6	233	0.39
	7	240	0.14
DeoxyHbA in glycerol/water	1	195	0.09
	2	202	0.16
	3		
	4	218	0.07
	5	225	0.15
	6	235	0.31
	7	242	0.22

suggest a 1:1 correspondence between the CS of the proximal part of the deoxygenated and the distal part of the ligated protein, which relates CS(A_0) to CS(SL_{Mb3}), CS(A_1) to CS(SL_{Mb2}), and CS(A_3) to CS(SL_{Mb1}). Differences in corresponding ratios may be due to different intrinsic intensities of the $\nu_{Fe\text{-}His}$ SLs or/and different occupations of the above CS in the ligated and unligated conformation.

In view of this interpretation the $\nu_{Fe\text{-}His}$ band of horse heart Mb measured at 10 K is indicative of a predominant CS(A_0) ($I(SL_{Mb3})/I(SL_{Mb2}) = 5.6$ and $I(SL_{Mb1})/I(SL_{Mb2}) < 10^{-2}$, cf. Table 6 and Fig. 10 *c*). Indeed this parallels measurements on the IR(CO) band of sperm whale Mb at the same temperature, which yields $A_0/A_1 \approx 2.0$. and $A_3/A_1 < 10^{-2}$ (Ansari et al., 1987).

Morikis and Champion (1989) have attributed A_0 and A_1 of MbCO to an open and a closed conformation of the heme pocket, respectively. More recent kinetic experiments from the same laboratory seem to corroborate this notion (Champion, 1992). Replacing the distal histidine by glycine causes a more open heme pocket thus giving rise to dominant SLs A_0 in the CO- and SL_{Mb3} in the $\nu_{Fe\text{-}His}$ band. If methionine is chosen as substituent for His^{E7}, the open and closed conformation exhibit similar populations (cf. Fig. 11 *b*).

Conclusions drawn from the Raman data

From the large body of experimental data, which we have analyzed the following picture emerges. The Fe^{2+}-N_ϵ(His^{F8}) bond exists in various substates, which are indicated by the frequency of the corresponding sublines and are related to a conformational coordinate x. Changes of the tertiary and (in Hb) quaternary structure of the protein do not affect these substates, as indicated by the stability of the frequencies. The intensities of the SLs, however, changes significantly. We assume, that this is caused by a redistribution of the occupation of the above CS and also to a large extent by variations along a second conformational coordinate y, which is affected by structural changes in the protein. The latter effect is involved in the pH dependence of the $\nu_{Fe\text{-}His}$ SLs of deoxyHb trout IV as has recently been shown in our laboratory (Bosenbeck et al., 1992). Since the coordinate y is reactive to changes which do not affect x, we infer that it must belong to a lower tier in the hierachy of CS.

Possible assignments of x and y to structural coordinates of the heme-His^{F8} complex are discussed below.

First experiments on the charge transfer band III

The optical spectra of deoxyHbA and deoxyMb show a weak band at 760 nm, which exhibits a similar sensitivity to distortions of the proximal heme side as the $\nu_{Fe\text{-}His}$ band (Izuka

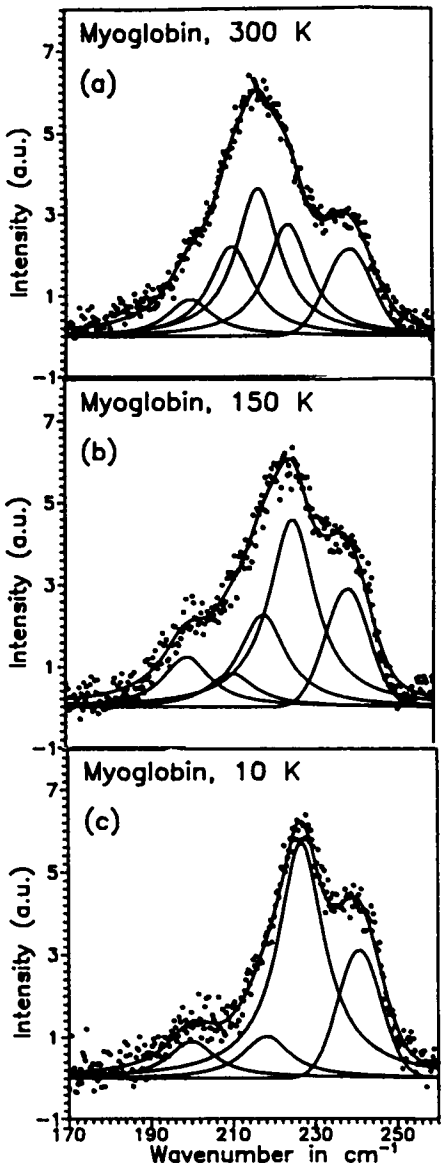

FIGURE 10 Band profile of the $\nu_{Fe\text{-}His}$ band of horse heart deoxyMb measured at $T = 300$ K (*a*), 150 K (*b*), and 10 K (*c*) in an aqueous solution. The profiles were decomposed into five sublines, three of which can be attributed to the $\nu_{Fe\text{-}His}$ mode.

TABLE 6 a: Band parameters derived from the analysis of $\nu_{Fe\text{-}His}$ band of horse heart deoxyMb measured at 300, 150, and 10 K in an aqueous solution. b: Band parameters derived from the analysis of $\nu_{Fe\text{-}His}$ band of sperm whale deoxyMb and the corresponding mutants Mb (Gly^{E7}) and Mb (Met^{E7}) measured at 300 K in an aqueous solution

T [K]	*Mj*	Ω_{Mj}	Γ_{Mj}	I_{Mj}/I_T
		cm^{-1}	cm^{-1}	
(a)				
300	p1	199	13	0.09
	1	211	13	0.20
	2	217	13	0.32
	3	225	13	0.24
	p2	240	16	0.15
150	p1	199	14	0.12
	1	210	14	0.08
	2	218	14	0.20
	3	225	14	0.44
	p2	239	15	0.16
10	p1	199	14	0.09
	1	210	14	
	2	218	14	0.11
	3	226	14	0.59
	p2	240	15	0.21
(b)				
Native sperm whale Mb	p1			
	1	206	12	0.06
	2	218	16	0.55
	3	226	16	0.18
	p2	240	20	0.21
Mb(Gly^{E7})	p1			
	1	208	12	0.04
	2	214	16	0.31
	3	224	16	0.56
	p2	244	18	0.09
Mb(Met^{E7})	p1			
	1	208	12	0.05
	2	218	14	0.36
	3	226	14	0.48
	p2	240	16	0.11

I_{Mj}, intensity of the *j*th SL; I_T, total intensity; p1 and p2 denote the lines resulting from vibrations different from $\nu_{Fe\text{-}His}$.

et al., 1972). This band, commonly referred to as band III, has been assigned to a charge transfer transition from the a_{2u} orbital of the porphyrin π system to the d_{z^2} state of Fe^{2+} (Eaton et al., 1978). In deoxyMb its intensity increases significantly toward cryogenic temperatures (Cordone et al., 1986, 1990). While in photoproducts of HbCO band III appears red-shifted by 11 nm after 10 ns and relaxes thereafter to its deoxy equilibrium value (<100 μs), it has fully relaxed after this time in Mb*CO (Sassaroli and Rousseau, 1987). This shift of the peak position depends on temperature (Ahmed et al., 1991). More recent experiments on Hb*CO revealed that in this species band III is red-shifted by 6 nm after 35 ps with respect to its equilibrium value at ambient temperature (Dunn and Simon, 1991) (in contrast to what has been observed by Sassaroli and Rousseau (1987), no relaxation was found between 35 ps and 60 ns). Moreover kinetic hole burning experiments indicate to the heterogeneity of this band. Its frequency position is correlated with the height of the energy barrier encountered by a (re)binding ligand (Campbell et al., 1987; Chavez et al., 1990; Steinbach et al., 1992). All this experiments strongly support the notion, that the energy position of band III is governed by the structure of the proximal heme side. Hence one expects, that it should be amenable to a similar analysis as that applied to the $\nu_{Fe\text{-}His}$ band.

We have therefore measured band III of deoxyHbA at room temperature and analyzed it by a band shape analysis. Owing to its apparent asymmetry (cf. Fig. 12) it cannot be fitted with only one single line. We found that the minimal model requires three subbands (SBs). A refinement is obtained by taking into account the contribution of two other, weak SBs. This fit is shown in Fig. 12. Apparently it is not

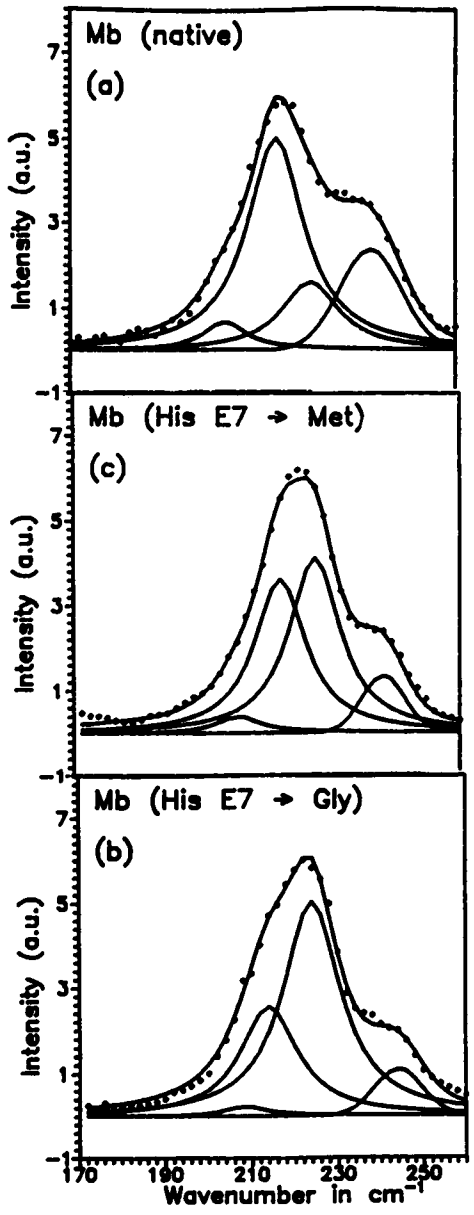

FIGURE 11 Band profile of the $\nu_{Fe\text{-}His}$ band of sperm whale deoxymyoglobin (*a*) and the corresponding mutants Mb (Gly^{E7}) (*b*) and Mb (Met^{E7}) (*c*, data from Morikis and Champion (1989). The profiles were decomposed into five sublines, three of which can be attributed to the $\nu_{Fe\text{-}His}$ mode.

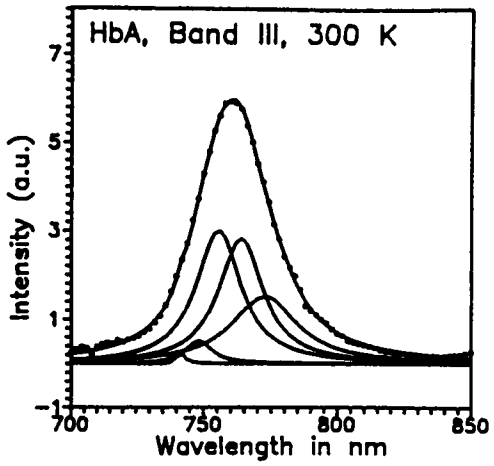

FIGURE 12 Profile of the optical charge transfer band III of deoxyHbA measured in a 65% glycerol/water mixture as described under Materials and Methods. The band was decomposed into five different subbands depicted by solid lines.

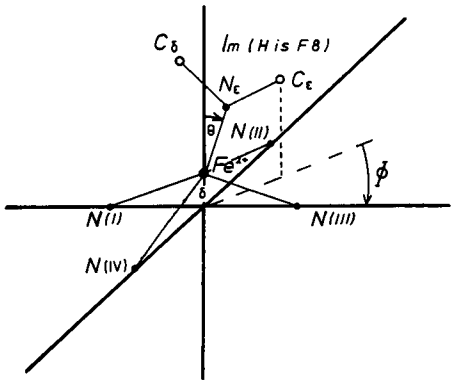

FIGURE 13 Schematic representation of the heme-$N_\epsilon(His^{F8})$ complex. N(I), N(II), N(III), and N(IV) are the pyrrole nitrogens, Θ is the tilt angle of the Fe^{2+}-$N_\epsilon(His^{F8})$ bond with respect to the heme normal, and ϕ is the azimuthal angle formed by the line N(I)-Fe^{2+}-N(III) and the projection of the imidazole on the heme.

possible to simply correlate the SBs of band III with the SLs of the corresponding $\nu_{Fe\text{-}His}$ (cf. Fig. 1), but as a first idea we may speculate that there is a mapping of the SLs observed in the $\nu_{Fe\text{-}His}$ band to those in band III.

Recently Srajer and Champion (1991) have suggested another model to understand the heterogeneity of band III in deoxyMb. They mapped a continuous Gaussian distribution of Fe^{2+} displacements onto the spectral position of band III by means of a quadratic coupling model (i.e., Ω(III) depends on the square of Fe^{2+} displacement). If one convolutes this distribution with a homogenous, Lorentzian band, an asymmetric band shape is obtained (Srajer et al., 1986). To further account for the temperature dependence of the width of band III the authors also assumed, that low frequency modes of the heme are coupled to the corresponding optical transition (Schomaker, 1987).

It is important to note that the analysis of Srajer and Champion (1991) is based on the assumption, that the position of band III is entirely determined by the iron displacement δ. For reasons given below we believe that this may be an oversimplification.

Possible assignments of the protein coordinates *x* and *y*

In parallel to other investigations (Bosenbeck et al., 1992; Friedman et al., 1990; Ahmed et al., 1991) this study shows that changes in the intensity of $\nu_{Fe\text{-}His}$ SLs may occur without

significant variations in their frequencies. Friedman et al. (1990) have recently proposed a simple model, which modifies an earlier proposal by Bangcharoenpaurpong et al. (1984). They relate the frequency of the $\nu_{Fe\text{-}His}$ lines to the tilt angle Θ formed by the Fe^{2+}-$N_\epsilon(His^{F8})$ bond with respect to the heme normal (cf. the schematic representation in Fig. 13). They argue that an increase in Θ causes the frequency to decrease, but in parallel the intensity to increase. Furthermore a change in the azimuthal angle ϕ does not affect the frequency but causes an increase in intensity with decreasing ϕ (Fig. 13). This model is based on the assumption, that the Soret excitation of the $\nu_{Fe\text{-}His}$ mode is determined by an overlap of the d_{z^2}-σ orbital (a_{1g}) of the Fe-$N_\epsilon(His^{F8})$ bond with the π^* orbitals (e_g) of the pyrrole nitrogens N(I) and N(III) (Fig. 13). Furthermore it is assumed that alterations of ϕ affect the π-π interaction between Fe^{2+} and $N_\epsilon(His^{F8})$ rather than their σ orbitals (Scheidt and Chipman, 1986), in such a way that the frequency of the Fe^{2+}-$N_\epsilon(His^{F8})$ remains unaffected. Thus this model identifies x with Θ and y with ϕ.

Chaudhury et al. (1992) have used this model to explain the heterogeneity of the $\nu_{Fe\text{-}Im}$ band of photo-reduced Fe(II)-octaethylporphyrin and Fe(II)-protoporphyrin IX-dimethylester complexes with 2-methylimidazole and 1,2-dimethylimidazole. This lead them to the suggestion that the corresponding Fe^{2+}-N_ϵ(Im) bonds exists in two conformations, one of which exhibits an upright and the other a tilted configuration with respect to the porphyrin normal.

Bosenbeck et al. (1992) successfully employed this model to rationalize the pH dependence of the $\nu_{Fe\text{-}His}$ SLs of deoxyHb-trout IV. They assumed that the protonation of Bohr groups changes the azimuthal angle ϕ without affecting the corresponding tilt angle. Therefore the intensities of the SLs become pH-dependent. Moreover this model is consistent with results emerging from most recent Raman dispersion studies on the v_4 mode of deoxyHb-trout IV (Schweitzer-Stenner et al., 1993), which revealed that strong asymmetric perturbations of the pyrrole nitrogens depend on pH in a similar way as the intensities of the $\nu_{Fe\text{-}His}$ Sls. Indeed one would expect that a decrease in ϕ causes a larger perturbation of N(I) and N(III) owing to the repulsive interactions between the pyrrole nitrogens and the imidazole of the proximal His^{F8} (cf. Schweitzer-Stenner and Dreybrodt (1992) for a more detailed analysis of this type of heme-protein interaction).

Even though the coupling model of Friedman et al. (1990) provides a reasonable and consistent description of a large body of Raman data (including our own results), some shortcomings and inconsistencies should not be overlooked. First, it cannot explain why the $\nu_{Fe\text{-}His}$ band of deoxyMb peaks at 218 cm^{-1} even though the tilt angle of its Fe-$N_\epsilon(His^{F8})$ bond is smaller (2°) than in deoxyHbA (9° in the α- and 6° in the β-subunit) (Fermi et al., 1984; Phillips, 1981). Second, the physical relationship between geometric parameters of the Fe-$N_\epsilon(His^{F8})$ complex and the vibronic coupling determining the intensities of the $\nu_{Fe\text{-}His}$ SLs remains unclear. Why, for instance, is the $\nu_{Fe\text{-}His}$ band not detectable in oxyMb, where the proximal imidazole eclipses the N(I)-Fe-N(III) line (i.e., $\phi = 0$) (Phillips, 1980)[1]

Some of these problems can be resolved by a model recently suggested by Stavrov (1993). It considers mixing of the a_{2u} orbitals of the porphyrin macrocycle and the antibonding d_{z^2}-σ_L orbitals of the Fe^{2+}-$N_\epsilon(His^{F8})$ bond by pseudo Jahn-Teller coupling (Bersuker and Stavrov, 1988), which is induced by out-of plane modes of A_{2u} symmetry. In a pentacoordinated Fe-porphyrin this coupling is affected by an axial-ligand crystal field of symmetry A_{2u} for $\Theta = 0$. This field stabilizes the high spin configuration of Fe^{2+} and causes its out of plane displacement δ (Fig. 11). The overlap between $a_{2u}(p)$ and $d_{z^2}(Fe)$ orbitals (the latter transforms like A_{1g} in D_{4h}) increases with increasing δ. Therefore the Fe-$N_\epsilon(His^{F8})$ vibration is coupled to the electronic states of the porphyrin macrocycle. In the B states, for instance, the A_{2u} population decreases. This gives rise to a reduction of the Fe-$N_\epsilon(His^{F8})$ bond and may also cause a decrease of the corresponding Fe^{2+} displacement δ. As a consequence the adiabatic potential minimum in the excited state moves with respect to the ground state along these coordinates thus giving rise to Raman intensity of the $\nu_{Fe\text{-}His}$ mode.

The above model does not explicitly consider, that δ is also determined by repulsive interactions between the imidazole and the pyrrole nitrogens (Olafson and Goddard, 1977; Gellin and Karplus, 1977; Warshel, 1977; Schweitzer-Stenner et al., 1993; Schweitzer-Stenner and Dreybrodt, 1992). Ab initio calculations by Olafson and Goddard (1977) have suggested, that this type of interaction governs the Fe^{2+} displacement δ, which in this case depends on the tilt angle Θ. This calculation, however, neglects the π-conjugated electronic subsystem of the porphyrin. It only considers four NH_2 groups in a plane to represent the porphyrin ligands of the iron. Thus it underestimates the electronic contributions to δ.

Stavrov's model relates the $\nu_{Fe\text{-}His}$ frequency to δ and Θ, because an increase in δ and a decrease of Θ give rise to a larger population of the antibonding d_{z^2}-σ_L orbital thus reducing the frequency of the $\nu_{Fe\text{-}His}$ mode (Stavrov, 1993; Stavrov and Kushkuley, 1993). This is consistent with the Fe-His^{F8} geometry in deoxyHbA, where δ is larger in the α- than in the β-subunits. It also qualitatively accounts for the δ values of some Fe-protoporphyrin derivatives (Hori and Kitagawa, 1980). Finally it may explain the situation in deoxyMb, where δ and Θ are smaller than in the HbA subunits (Phillips, 1981). This reduction in δ would be expected to

[1]The tilt angle Θ of deoxyMb was calculated from the crystal structure coordinates of Phillips (1981). These data are obtained with 1.6-Å resolution and should therefore be considered as being more accurate than the data reported in Takano's study (1977), which were derived with 2.6-Å resolution. It is important to realize that the geometric parameters of the Fe^{2+}-His^{F8} complex emerging from these studies are quite different. While Takano (1977) reports $\delta = 0.42$ Å, $\Theta = 11°$, and $\phi = 19°$, the coordinates provided by Phillips (1981) suggest that $\delta = 0.31$ Å, $\Theta = 2°$, and $\phi = 12°$. Since the heme in Phillips' structure is nonplanar and asymmetrically distorted, the latter values must be considered to be average ones.

increase the $\nu_{Fe\text{-}His}$ frequency, but this may be partially compensated by the small tilt angle Θ. As a consequence the apparent $\nu_{Fe\text{-}His}$ frequency of deoxyMb appears between those of the deoxyHbA subunits.

In order to rationalize those changes in intensity which do not coincide with alterations of the corresponding frequency Stavrov (1993) suggested that in a distinct heme protein the decrease in frequency upon increasing δ may be reduced or compensated either by strengthening of the hydrogen bond between His^{F8} and Val^{F4}, which has been shown to exist in deoxyMb (Takano, 1977) and in both subunits of deoxyHb (Liddington et al., 1988) or by a simultaneous increase of the tilt angle Θ. In this case the intensity may increase without significant changes of the corresponding frequency.

We feel that at present a final model cannot be presented. Further experiments on structurally well defined model substances are necessary. In the following we tentatively outline some aspects of both models which we think must be included in a final model:

(i) We believe that Stavrov (1993) is right in assuming that a resonance enhancement of the $\nu_{Fe\text{-}His}$ mode requires a significant out-of-plane displacement of Fe^{2+}. To our knowledge no heme protein or porphyrin-imidazole model complex was found which exhibits a $\nu_{Fe\text{-}His}$ band, when the iron is in a planar or nearly planar configuration. Moreover, one has to take into account that the energy difference between $e_g(\pi)$ and $d_{z^2}(Fe)$ states is by a factor of 4 larger than that between $d_{z^2}(Fe)$ and $A_{2u}(\pi)$ (Zerner et al., 1966). As a consequence one expects that the coupling mechanism giving rise to the Fe^{2+} out-of-plane displacement, i.e., the A_{2u}-type pseudo Jahn-Teller interaction between $a_{2u}(P)$ and $d_{z^2}(Fe)$, should be more effective than the interaction between $e_g(\pi)$ and $d_{z^2}(Fe)$ (E_g-type), which is determined by the tilt angle Θ.

(ii) It should not be overlooked that all three coordinates under discussion, namely Θ, ϕ and δ are most probably coupled with each other. Increasing the tilt angle Θ and/or decreasing the azimuthal angle enhances the repulsive heme-imidazole interaction which can be at least partially compensated by a larger Fe^{2+} displacement. On the other hand an increase in δ may force the imidazole into a more tilt position because of its interaction with the F helix (Gellin and Karplus, 1977; Warshel, 1977).

(iii) Alterations in the $\nu_{Fe\text{-}His}$ frequency may be caused by changes of both Θ and δ. Large δ values reflect a strong mixing of a_{2u} orbitals into d_{z^2} which gives rise to a decrease in frequency (Stavrov, 1993). While Friedman et al. (1990) assumed that an increase in Θ reduces the frequency, most recent extended Hückel calculations (Stavrov and Kushkuley, 1993) suggest an opposite relationship.

(iv) As outlined above, Stavrov's model (1993) predicts that the intensity of $\nu_{Fe\text{-}His}$ may depend on the reduction of the Fe^{2+} displacement δ in the excited B state. A decrease in δ, however, increases the repulsive interaction between the proximal imidazole and the heme nitrogens. To relax the thus imposed strain, the imidazole must move into a less tilted (smaller Θ) or less eclipsed position (larger ϕ) with respect to the heme. The first process requires some flexibility in the structure of the heme environment. It may therefore be operative in deoxyMb and to a minor extent in the β-subunits of deoxyHb, but it becomes unlikely in the α-subunits of deoxyHbA, where the protein is tightly packed around the heme (Liddington et al., 1988). A increase of the azimuthal angle, however, encounters significantly less steric hindrance by the protein than a reduction of Θ. Hence we expect, that the imidazole mainly increases its azimuthal angle in the B state. The smaller the ϕ value in the ground state the larger is the gain in energy provided by this conformational change. Thus one would understand how the ϕ angle, as suggested by Friedman's model (1990) can affect the intensity of the $\nu_{Fe\text{-}His}$ band.

Such a combination of Stavrov's and Friedman's models can be used to explain the $\nu_{Fe\text{-}His}$ intensity of deoxyMb, which is significantly stronger than that of the corresponding bands of the deoxyHb subunits (Rousseau and Friedman, 1988). This difference cannot be explained in terms of different Fe^{2+} displacements, because δ is smaller in deoxyMb than in deoxyHb (Fermi et al., 1984; Phillips, 1981). The azimuthal angle ϕ, however, is smaller in deoxyMb than in the unligated HbA subunits.

Scheidt and Chipman (1986) have demonstrated by extended Hückel calculations that changes in the azimuthal angle ϕ do not significantly affect the Fe-$N_\epsilon(His^{F8})$ σ bond, which governs the frequency of the $\nu_{Fe\text{-}His}$ stretch. This has been confirmed by the quantum chemical study reported by Stavrov and Kushkuley (1993). Thus ϕ remains a candidate for the intensity determining coordinate y, but as outlined above it seems likely that it affects the intensity in a more indirect way.

Some final remarks should be given on the relationship between band III and the $\nu_{Fe\text{-}His}$ band. Certainly the integrated absorption of the former and the intensity of the latter depend on the iron displacement δ (Zerner et al., 1966; Stavrov, 1993). Most models suggest that the wavelength position of band III is entirely determined by δ (Steinbach et al., 1992; Srajer and Champion, 1991; Champion, 1992), but this seems to be unlikely because tilting of Fe^{2+}-$N_\epsilon(His^{F8})$ causes electronic interactions between d_{z^2} and d_π orbitals, by which the energies of both can be altered (Stavrov, private communication). Ahmed et al. (1991) showed that below 70 K band III of Mb^*CO shifts its wavelength position as a function of temperature, whereas the $\nu_{Fe\text{-}His}$ mode solely changes its intensity. This shows that the latter is determined by a parameter which does not affect the position of band III. In accordance with Friedman's model the azimuthal angle seems to be an appropriate candidate for this, because changes in ϕ do not alter the symmetry of the Fe-Im(F8) complex and should therefore not significantly affect the energy levels of the iron d orbitals. The results of Ahmed et al. (1992) further suggest that the wavelength position of band III and the frequency of $\nu_{Fe\text{-}His}$ differ in their dependence on δ and Θ. If one extends this observations to

deoxyHb, one can understand why in this study we did not find a simple correlation between the subbands of band III and the SLs of $\nu_{Fe\text{-}His}$.

We gratefully acknowledge that part of this work is supported by a grant from the Deutsche Forschungsgemeinschaft (DFG). We would like to thank Dr. Solomon Stavrov for helpful discussions and for providing a reprint of his paper, Dr. G. Ulrich Nienhaus for calling our attention to newest crystallographic data on deoxyMb observed by S. E. V. Phillips (cf. Phillips, 1981), and Dr. George Phillips, Jr. for providing us the respective atomic coordinates. Finally we thank Dr. Eberhard Schlodder and Martin Gergeleit from the Max-Volmer-Institut of the Technical University of Berlin for enabling us to measure band III of deoxyHbA.

REFERENCES

Ahmed, A. M., B. F. Campbell, D. Caruso, M. R. Chance, M. D. Chavez, S. H. Courtney, J. M. Friedman, I. E. T. Iben, M. R. Ondrias, and M. Yang. 1991. Evidence for proximal control of ligand specificity in heme proteins: absorption and Raman studies of cryogenically trapped photoproducts of ligand bound myoglobins. *Chem. Phys.* 158:239–351.

Ansari, A., J. Berendzen, S. F. Bowne, H. Frauenfelder, I. E. T. Iben, T. B. Sauke, E. Shysamunder, and R. D. Young. 1985. Protein States and Protein Quakes. *Proc. Natl. Acad. Sci. USA.* 85:5000–5004.

Ansari, A., J. Berendzen, D. Braunstein, B. R. Cowen, H. Frauenfelder, M. K. Kong, I. E. T. Iben, J. Johnson, P. Ormos, T. B. Sauke, R. Scholl, A. Schulte, P. J. Steinbach, R. D. Vittitow, and R. D. Young. 1987. Rebinding and relaxation in the myoglobin pocket. *Biophys. Chem.* 26:337–355.

Baldwin, J. L., and C. Chothia. 1979. Haemoglobin, the structural changes related to ligand binding and its allosteric mechanism. *J. Mol. Biol.* 129: 175–200.

Bangcharoenpaurpong, O., K. T. Schomaker, and P. M. Champion. 1984. A resonance Raman investigation of myoglobin. *J. Am. Chem. Soc.* 108: 1163–1167.

Bersuker, I. B., and S. S. Stavrov. 1988. Structure and properties of metalloporphyrins and hemoproteins: the vibronic approach. *Coord. Chem. Rev.* 88:1–68.

Bosenbeck, M., R. Schweitzer-Stenner, and W. Dreybrodt. 1992. pH-induced conformational changes of the Fe^{2+}-N_ϵ(His F8) linkage in deoxyhemoglobin trout IV detected by the Raman active Fe^{2+}-N_ϵ(His F8) stretching mode. *Biophys. J.* 61:31–41.

Campbell, B. F., M. R. Chance, and J. M. Friedman 1987. Linkage of functional and structural heterogeneity in proteins: dynamic hole burning in carboxymyoglobin. *Science (Wash. DC).* 238:373–376.

Caughey, W. S., H. Shimada, M. G. Choc, and M. P. Tucker. 1981. Dynamic protein structures: infrared evidence for four discrete, rapidly interconverting conformers at the carbon monoxide binding site of bovine heart myoglobin. *Proc. Natl. Acad. Sci. USA.* 78:2903–2907.

Champion, P. M. 1988. Cytochrome P450 and the transform analysis of heme protein Raman spectra. *In* Biological Application on Raman Spectroscopy. T. G. Spiro, editor. John Wiley & Sons, New York. 249–292.

Champion, P. M. 1992. Raman and kinetic studies of myoglobin structure and dynamics. *J. Raman Spectrosc.* 23:557–567.

Chaudhury, N. K., G. S. S. Saini, and A. L. Verma. 1992. Stereochemical aspects of axial ligation in ferrous iron porphyrins probed by resonance Raman spectroscopy. *Spectrochim. Acta.* 48A:1589–1599.

Chavez, M. D., S. H. Courtney, M. R. Chance, D. Kiula, J. Nocek, B. M. Hofman, J. M. Friedman, and M. R. Ondrias. 1990. Structural and functional significance of inhomogenous line broadening of band III in hemoglobin and Fe-Mn hybrid hemoglobin. *Biochemistry.* 29:4844–4852.

Chiancome, E., J.-E. Norne, S. Forsen, and E. Antonini. 1983. Chloride binding to hemoglobin as studied by nuclear magnetic quadrupole relaxation. *In* Hemoglobin and Oxygen Binding. C. Ho, editor. MacMillan Press, London. 263–268.

Cordone, L., A. Cupane, M. Leone, and E. Vitrano. 1986. Optical absorption spectra of deoxy and oxyhemoglobin in the temperature range 300–20 K. *Biophys. Chem.* 24:259–275.

Cordone, L., A. Cupane, M. Leone, and E. Vitrano. 1990. *Biopolymers.* 29:639–643.

Doster, W., S. Cusack, and W. Petry. 1989. Dynamical transition of myoglobin revealed by inelastic neutron scatterin. *Nature (Lond.).* 337:754–756.

Dunn, R. C., and J. D. Simon. 1991. Picosecond study of the near infrared absorption band of hemoglobin after photolysis of carbonmonoxyhemoglobin. *Biophys. J.* 60:884–889.

Eaton, W. A., L. K. Hanson, P. J. Stephens, J. C. Sutherland, and J. B. R. Dunn. 1978. Optical spectra of oxy- and deoxyhemoglobin. *J. Am. Chem. Soc.* 100:4991–5001.

Elber, R., and M. Karplus. 1987. Multiple conformational states of proteins: a molecular dynamics analysis of myoglobin. *Science (Wash. DC).* 235: 318–321.

Fermi, G., M. F. Perutz, B. Shaanan, and R. Fourme. 1984. Human deoxyhaemoglobin at 1.74 Å resolution. *J. Mol. Biol.* 175:159–174.

Friedman, J. M. 1985. Structure, dynamics and reactivity in hemoglobin. *Science (Wash. DC).* 228:1274–1280.

Friedman, J. M., B. F. Campbell, and R. W. Noble. 1990. A possible new control mechanism suggested by resonance Raman spectra from a deep ocean fish hemoglobin. *Biophys. Chem.* 37:43–59.

Frauenfelder, H., F. Parak, and R. D. Young. 1988. Conformational substates in proteins. *Annu. Rev. Biophys. Biophys. Biochem.* 17:451–479.

Gellin, B. R., and Karplus, M. 1977. Mechanism of tertiary structural changes in hemoglobin. *Proc. Natl. Acad. Sci. USA.* 74:1789–1793.

Grinvald, A., and I. Z. Steinberg. 1974. On the analysis of fluorescence decay kinetics by the method of least square. *Anal. Biochem.* 59:583–598.

Hori, H., and T. Kitagawa. 1980. Iron-ligand stretching band in the resonance Raman spectra of ferrous iron porphyrin derivatives. Importance as a probe for quaternary structure of hemoglobin. *J. Am. Che. Soc.* 102: 3608–3613.

Iben, I. E. T., D. Braunstein, W. Doster, H. Frauenfelder, H. K. Hong, J. B. Johnson, S. Luck, P. Ormos, A. Schulte, P. Steinbach, A. Xie, and R. D. Young. 1989. Glassy behaviour of a protein. *Phys. Rev. Lett.* 62:1916–1919.

Izuka, T., H. Yamamoto, M. Kotani, and Y. Yonetani. 1972. Low temperature photodissociation of heme proteins: carbon monoxide complex of myoglobin and hemoglobin. *Biochim. Biophys. Acta.* 372:126–139.

Jung, C., and F. Marlow. 1987. Dynamic behaviour of the active site structure in bacterial cytochrome P-450. *Stud. Biophys.* 3:241–251.

Jung, C., R. Scholl, H. Frauenfelder, and G. Hui Bon Hua. 1992. Structural multiplicity in the active center of cytochrome P-450. *In* Cytochrome P-450: Biochemistry and Biophysics. A. I. Archakov and G. I. Bachmanova, editors. Joint Stock Company, Moscow. 33–38.

Kitagawa, T. 1988. Heme protein structure and the iron histidine stretching mode. *In* Biological Application on Raman Spectroscopy. T. G. Spiro, editor. John Wiley & Sons, New York. 97–132.

Liddington, R., Z. Derewenda, G. Dodson, and D. Harris. 1988. Structure of the liganded T state of haemoglobin identifies the origin of cooperative oxygen binding. *Nature (Lond.).* 331:725–728.

Makinen, M. W., R. A. Houtchens, and W. S. Caughey. 1979. Structure of carboxymyoglobin in crystals and in solution. *Proc. Natl. Acad. Sci. USA.* 76:6042–6046.

Matsukawa, S., K. Mawatari, Y. Yoneyama, and T. Kitagawa. 1984. Correlation between iron histidine stretching frequencies and oxygen affinities of hemoglobins. A continuous strain model. *J. Am. Chem. Soc.* 107: 1108–1116.

Mayo, K. H., D. Kucheida, F. Parak, and J. C. W. Chien. 1983. Structural dynamics of human deoxyhemoglbin and hemochrome investigated by nuclear gamma resonance absorption (Mößbauer) spectroscopy. *Proc. Natl. Acad. Sci. USA.* 80:5294–5296.

Morikis, D., P. M. Champion, B. A. Springer, and S. G Sligar. 1989. Resonance Raman investigations of site-directed mutants of myoglobin: effects of distal histidine replacement. *Biochemistry.* 28:4791–4800.

Nagai, K., and T. Kitagawa. 1979. Differences in Fe(II)-N_ϵ(His F8) stretching frequencies between deoxyhemoglobin in two alternative quaternary structures. *Proc. Natl. Acad. Sci. USA.* 77:2033–2037.

Nagai, K., T. Kitagawa, and H. Morimoto. 1980. Quaternary structures and low frequency molecular vibrations of haems of deoxy- and oxyhaemoglobin studied by resonance Raman scattering. *J. Mol. Biol.* 136:217–289.

Nagai, M., Y. Yoneyama, and T. Kitagawa. 1989. Characteristics in tyrosine coordinations of four hemoglobins M probed by resonance Raman spectroscopy. *Biochemistry.* 28:2418–2422.

Nagai, K., K. Fushitani, G. Miyazaki, K. Ishimori, T. Kitagawa, Y. Wada, H. Morimoto, I. Morishima, D. T.-b. Shih, and J. Tame. 1991. Site directed mutagenesis in haemoglobin. Functional role of tyrosine-42 (C7)α at the α1-β2 interface. *J. Mol. Biol.* 218:769–778.

Nienhaus, G. U., J. Heinzl, E. Huegens, and F. Parak. 1989. Protein crystal dynamics studied by time-resolved analysis of x-ray diffuse scattering. *Nature (Lond.)*. 338:665–666

Nienhaus, G. U., H. Frauenfelder, and F. Parak. 1992. Structural fluctuations in glass-forming liquids: Möβbauer spectroscopy on iron in glycerol. *Phys. Rev.* B3:3345–3350.

Nienhaus, G. U., J. Mourant, and H. Frauenfelder. 1992. Spectroscopic evidence for conformational relaxation in myoglobin. *Proc. Natl. Acad. Sci. USA*. 89:2902–2906.

Olafson, B. D., and W. A. Goddard III. 1977. Molecular description of dioxygen bonding in hemoglobin. *Proc. Natl. Acad. Sci. USA*. 74:1315–1319.

Ondrias, M. R., D. L. Rousseau, T. Kitagawa, M. Ikeda-saito, T. Inubushi, and T. Yonetani. 1982. Quaternary structure changes in iron-cobalt hybrid hemoglobins detected by resonance Raman scattering. *J. Biol. Chem.* 10:8766–8770.

Ormos, P., D. Braunstein, H. Frauenfelder, M. K. Hong, A.-L. Lin, T. B. Sauke, and R. D. Young. 1988. Orientation of carbon monoxide and structure-function relationship in carbonmonoxymyoglobin. *Proc. Natl. Acad. Sci. USA*. 85:8492–8496.

Ormos, P., A. Ansari, D. Braunstein, B. R. Cowen, H. Frauenfelder, M. K. Hong, I. E. T. Iben, T. B. Sauke, P. J. Steinbach, and R. D. Young. 1990. Inhomogenous broadening in spectral bands of carbonmonoxymyoglobin. The connection between spectral and functional heterogeneity. *Biophys. J.* 57:191–200.

Parak, F., E. W. Knapp, and D. Kucheida. 1982. Protein dynamics Möβbauer spectroscopy on deoxymyoglobin crystals. *J. Mol. Biol.* 161:177–194.

Perutz, M. F. 1989. Mechanism of cooperativity and allosteric regulation in proteins. *Q. Rev. Biophys.* 22:139–236.

Phillips, S. E. V. 1981. The x-ray structure of deoxyMb (pH = 8.5) at 1.4 Å resolution. Brookhaven Protein Data Bank.

Phillips, S. E. V. 1980. Structure and refinement of oxymyoglobin at 1.6 Å resolution. *J. Mol. Biol.* 142:531–554.

Rodgers, K. R., C. Su, S. Subramaniam, and T. G. Spiro. 1992. Hemoglobin R→T structural dynamics from simultaneous monitoring of tyrosine and tryptophan time-resolved UV resonance Raman signals. *J. Am. Chem. Soc.* 114:3697–3709.

Rousseau, D. L, and J. M. Friedman. 1988. Transient and cryogenic studies of photodissociated hemoglobin and myoglobin. *In* Biological Application on Raman Spectroscopy. T. G. Spiro, editor. John Wiley & Sons, New York. 133–216.

Russu, I. R., S.-S. Wu, N. T. Ho, G. W. Kellog, and C. Ho. 1989. A proton nuclear magnetic resonance investigation of the anion Bohr effect of human adult hemoglobin. *Biochemistry.* 28:5298–5306.

Sassaroli, M., and D. L. Rousseau. 1987. Time dependence of near infrared spectra of photodissociated hemoglobin and myoglobin. *Biochemistry.* 26:3092–3098.

Schomaker, K. T. 1987. Absorption, resonant Rayleigh and resonant Raman properties of cytochrome *c*. PhD thesis. Notheastern University, Boston.

Scheidt, W. R., and D. M. Chipman. 1986. Preferred orientation of imidazole ligands in metalloporphyrins. *J. Am. Chem. Soc.* 108:1163–1167.

Schweitzer-Stenner, R., and W. Dreybrodt. 1989. An extended Monod-Wyman-Changeaux model expressed in terms of the Herzfeld-Stanley formalism applied to oxygen and carbonmonoxide binding curves of hemoglobin trout IV. *Biophys. J.* 55:691–701.

Schweitzer-Stenner, R., and W. Dreybrodt. 1992. Investigation of haem-protein coupling and structural heterogeneity in myoglobin and haemoglobin by resonance Raman spectroscopy. *J. Raman Spectrosc.* 23:539–550.

Schweitzer-Stenner, R., M. Bosenbeck, and W. Dreybrodt. 1993. Raman dispersion spectroscopy probes heme distortions in deoxyHb-trout IV involved in its T-state Bohr effect. *Biophys. J.* 64:1194–1209.

Srajer, V., and P. M. Champion. 1991. Investigation of optical line shapes and kinetic hole burning in myoglobin. *Biochemistry.* 30:7390–7402.

Srajer, V., K. T. Schomaker, and P. M. Champion. 1986. Spectral broadening in biomolecules. *Phys. Rev. Lett* 57:1267–1270.

Stavrov, S. S. 1993. The effect of iron displacement out of the porphyrin plane in the resonance Raman spectra of heme proteins and iron porphyrins. *Biophys. J.*, in press.

Stavrov, S. S., and B. Kushkuley. 1993. Dependence of the iron-histidine frequency of deoxy heme proteins on the structure of its active center: quantum chemical study. *In* Proceedings of the Fifth European Conference on the Spectroscopy of Biological Molecules. T. Theophanides, editor. Athens, Greece. Kluwer, Amsterdam. 305–306.

Steinbach, P. J., A. Ansari, J. Berendzen, D. Braunstein, K. Chu, B. R. Cowen, D. Ehrenstein, H. Frauenfelder, J. B. Johnson, D. C. Lamb, S. Luck, J. R. Mourant, G. U. Nienhaus, P. Ormos, R. Philipp, A. Xie, and R. D. Young. 1991. Ligand binding to heme proteins: connection between dynamics and function. *Biochemistry.* 30:3988–4001.

Takano, T. 1977. Structure of myoglobin refined at 2.0 Å resolution. II: Structure of deoxymyoglobin from sperm whale. *J. Mol. Biol.* 142:531–554.

Terner, J., T. G. Spiro, M. Nagumo, M. F. Nicol, and M. A. El-Sayed. 1980. Resonance Raman spectroscopy in the picosecond time scale: the carboxyhemoglobin photointermediate. *J. Am. Chem. Soc.* 102:3238–3239.

Tsubaki, M., K. Shinzawa, and S. Yoshikawa. 1992. Effects of crystallization on the heme-carbon monoxide moiety of bovine heart cytochrome c oxidase carbonyl. *Biophys. J.* 63:1564–1571.

Warshel, A. 1977. Energy-structure correlations in mettalloporphyrins and the control of oxygen binding by hemoglobin. *Proc. Natl. Acad. Sci. USA.* 74:1789–1793.

Zerner, M., M. Gouterman, and H. Kobayashi. 1966. Porphyrins. VII. Extended Hückel calculation on iron complex. *Theoret. Chim. Acta.* 6:363–400.

Zhu, L., J. T. Sage, A. A. Rigos, D. Morikis, and P. M. Champion. 1992. Conformational interconversion in protein crystals. *J. Mol. Biol.* 224: 207–215.